CONCRETE RESEARCH LETTERS

www.crl.issres.net

Vol. 2 (3) – Sep. 2011

Mechanisms of Corrosion-Induced Cracks in Concrete

M. Ohtsu[1c] and F. A. K. M. Uddin[2]

[1]*Professor, Graduate School of Science & Technology, Kumamoto University, JAPAN*

[2]*Sr. Water Structural Design Engineer, BW Perunding, Kuala Lumpur-50460, MALAYSIA*

Abstract

Corrosion-induced cracks was simulated in expansion tests. Kinematical mechanisms of micro-cracks were identified by the SiGMA analysis of acoustic emission (AE). By applying the boundary element method (BEM), extension of the corrosion-induced crack in an arbitrary direction was analyzed. It is demonstrated that extension of the corrosion-induced crack is governed by the mode-I failure, although all kinds of micro-cracks are observed in results of AE analysis.

Keywords: Corrosion-induced crack; Acoustic emission; Boundary element method; Stress intensity factor; Fracture Mechanics.

1. Introduction

Because of severe environmental effects, concrete structures can deteriorate and are known to be not maintenance-free. One of the critical deteriorations in concrete is a corrosion-induced cracking. From the physical point of view, the corrosion-induced crack could result from an accumulation process of micro-cracks, which create the fracture process zone as rationalized in fracture mechanics. Then, micro-cracks coalesce macroscopically to nucleate a tensile crack. According to fracture mechanics, cracks can nucleate in three distinct modes, namely tensile opening (mode I), in-plane shear (mode II) and out-of-plane shear (mode III). It is demonstrated that mode I plays a key role for crack extension in concrete, whereas the contribution of mode II and mode III remains unknown [1]. A theoretical analysis of AE waves could provide kinematic information on mechanisms at the meso-scale, because the moment tensor analysis [2]. At the macro-scale, crack propagation due to expansive pressure was previously analyzed on the basis of linear elastic fracture mechanics (LEFM) by the boundary element method (BEM) [3]. Focusing on mechanisms of crack extension, fracture modes of the corrosion-induced cracks are discussed at the meso- and at the macro-scales, introducing the normalized stress intensity factors [4].

[c] Corresponding Author: Masayasu Ohtsu
Email: ohtsu@gpo.kumamoto-u.ac.jp Telephone: +81 963423542 Fax: +81 963423507
© 2009-2012 All rights reserved. ISSR Journals

2. Meso-scale mechanisms by AE analysis

In order to study mechanisms of these corrosion-induced cracks at the meso-scale by AE analysis, SiGMA (**Si**mplified **G**reen's functions for **M**oment tensor **A**nalysis) procedure [2] is applied. The moment tensor is defined as the product of the elastic constants [N/m^2] and the crack volume [m^3], which leads to the moment in mechanics as a physical unit [Nm]. It is noted that cracks nucleate in distinct three modes in fracture mechanics, i.e., mode I, mode II and mode III. Rigorously speaking, they correspond to the ideal cases where vector **l** is parallel to vector **n** (mode I) or vector **l** is perpendicular to vector **n** (modes II and III). In a general case, two vectors are neither parallel nor perpendicular. It is noted that the three modes are closely related with stress singularity at the crack-tip, not explicitly associated with movements of crack planes.

The classification of a crack is performed by the eigen-value analysis of the moment tensor and a visualization procedure is developed. Crack movements are classified into tensile-crack, mixed-mode and shear-crack, of which models are given in Fig. 1. Here, an arrow indicates a crack motion vector , and a circular plate corresponds to a crack surface, which is perpendicular to a crack normal vector. Thus, a crack movement of each AE source is kinematically identified at the meso-scale. This procedure is applied to study corrosion-induced micro-cracking in an expansion test.

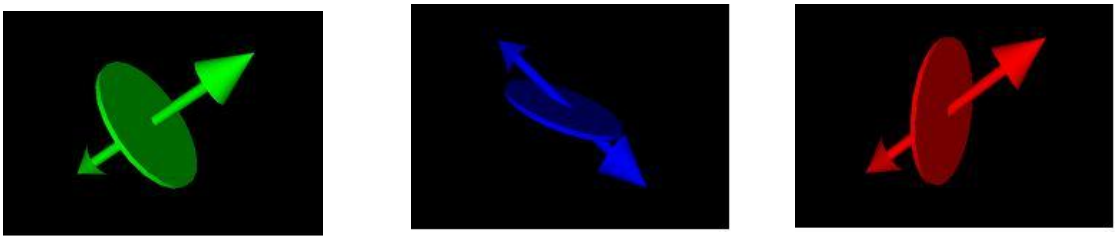

(a) tensile-crack (b) shear-crack (c) mixed-mode

Figure 1. VRML models for tensile-crack, shear-crack, and mixed-mode movements.

3. Macro-scale mechanisms by BEM analysis

Linear-elastic fracture mechanics (LEFM) can be applied to predict crack orientation under mixed-mode loading [3]. According to LEFM, the angle of crack initiation q is obtained from the maximum circumferential stress [5],

$$K_I \sin q + K_{II}(3\cos q - 1) = 0. \quad (1)$$

Here K_I and K_{II} are the stress intensity factors of the mode I and the mode II, which can be computed from the displacements on the crack-tip elements in the BEM analysis. Introducing the critical stress intensity factor K_{IC}, the initiation of crack extension is governed by,

$$\cos\frac{q}{2}\left(K_I \cos^2\frac{q}{2} - \frac{3}{2}K_{II}\sin q\right) = K_{IC}. \quad (2)$$

A crack trajectory at the macro-scale can be computed, automatically separating into two domains from a crack-tip. The procedure is applied to analyze crack extensions observed in the expansion test.

4. Experiment

In order to simulate the expansion caused by corrosion products, an expansion pressure was introduced by employing an expansive agent. The agent employed was dolomite paste (water: dolomite = 1: 2 by weight), which was inserted into a hole in a specimen. Concrete specimens of dimensions 250 mm x 250 mm x 100 mm with a hole of 30 mm diameter were tested. The hole

corresponds to the rebar location with 40 mm cover-thickness. The concrete mixture proportion was determined as water (W): cement (C): sand (S): gravel (G) = 0.5: 1.0: 2.41: 2.95 by weight. The maximum size of gravel was 20 mm. The compressive strength of concrete at 28-day standard curing was 37.9 MPa. The velocity of P wave was 4730 m/s and the modulus of elasticity was 29.7 GPa.

During the test, the expansive pressure was measured by using an embedded pressure-gauge. AE events were detected by a six-channel AE system. Six AE sensors (PAC, UT1000) were attached to the concrete specimen by means of silicone grease. Arrangement of AE sensors with AE equipments is shown in Figure 9. AE waves were amplified by 50dB with a preamplifier and detected when exceeding the threshold level of 50 dB. AE waveforms and parameters were recorded and analyzed by TRA212 AE system (PAC). Sampling time for recording AE waves was 1 μsec with 2048 words. P-wave velocity measured was applied to the SiGMA analysis.

5. Results and discussion

At the meso-scale, all types of crack movements were really mixed up according to the SiGMA analysis. It implies that micro-cracks are accumulated to create the fracture process zone, and then coalesce as macroscopic cracks (surface or diagonal). In other words, macro-cracks grow around the hole in concrete, after weakening occurs due to micro-cracks. Because the surface crack is short and tensile-crack movements were dominantly observed in the SiGMA analysis, extension mechanisms of the diagonal crack were analytically examined. At the macro-scale, from Eqs. 1 and 2, the contribution K_I and K_{II} can be obtained as the normalized stress intensity factors K_I/K_{IC} and K_{II}/K_{IC},

$$\frac{K_I}{K_{IC}} = \frac{1-3\cos\theta}{\cos^3\frac{\theta}{2}(1-3\cos\theta)-\frac{3}{2}\sin^2\theta\cos\frac{\theta}{2}}$$

$$\frac{K_{II}}{K_{IC}} = \frac{\sin\theta}{\cos^3\frac{\theta}{2}(1-3\cos\theta)-\frac{3}{2}\sin^2\theta\cos\frac{\theta}{2}}. \quad (3)$$

In order to estimate the contribution of K_I and K_{II}, the diagonal crack observed was selected and analysed. The normalized stress intensity factors in Eq. 3 were computed from the BEM analysis. In the analysis, new crack orientations q can be computed consecutively. These angles were substituted into Eq. 3. From visual observation, crack orientations on the concrete surface were directly measured and again substituted into Eq. 9 to compare with the analysis. At the meso-scale, normal vectors **n** to the crack surface can be derived from the SiGMA analysis. Consequently, only AE events near the diagonal crack were selected on the basis of their locations. The angle q was determined from a scalar product, $\cos q = (\mathbf{n_1}, \mathbf{n_2})$, of two normal vectors $\mathbf{n_1}$ and $\mathbf{n_2}$ of consecutive AE events. The procedure implies that only crack orientations are taken into account, as the directions of crack movements on the crack surface are neglected.

All results of the normalized stress intensity factors obtained are plotted in Fig. 2. It is found that the normalized stress intensity factors of mode I (K_I/K_{IC}) are always dominant, compared with those of mode II (K_{II}/K_{IC}). This implies that mode I failure occurs during the extension of the diagonal crack. At the macro-scale, the crack trajectory is observed as mode I in the experiments as well as performed in the BEM analysis. At the meso-scale, although all types of crack movements were observed in the SiGMA analysis, results also suggest generation of the mode-I failure, in the case that the crack orientation between consecutive events is taken into account only.

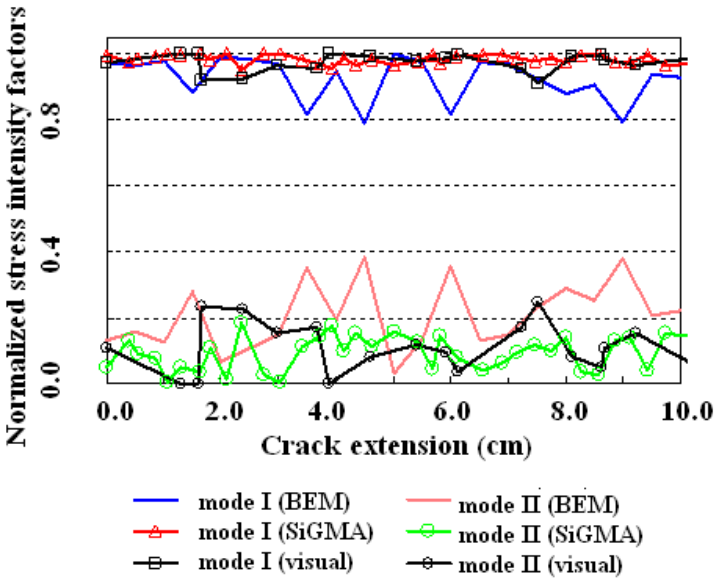

Figure 2. Normalized stress intensity factors.

6. Conclusion

(1) From the SiGMA analysis, all types of crack movements at the meso-scale were observed as to be mixed-up around the surface crack and the diagonal cracks. These results indicate that cracking movements at the meso-scale always consist of both opening and lateral (sliding) movements on the crack surface.
(2) At the macro-scale, a diagonal corrosion-induced crack was generated after the development of a surface crack, due to the pressure caused by the expansion. The crack trajectory was simulated by the BEM analysis, and was in reasonable agreement with that of the experiment.
(3) Based on the Erdogan-Sih criterion, the normalized stress intensity factors were examined. One diagonal crack was selected, and the factors were calculated from visual observation, the BEM analysis and the SiGMA analysis. All results are in good agreement. The mode I is always dominant. It leads to the conclusion that the extension of the corrosion-induced crack is primarily governed by the mode-I failure both at the meso-scale and the macro-scale.

References

[1] Lilliu, G. and van Mier, J. G. M. *3D Lattice-Type Fracture Model for Concrete*, Engineering Fracture Mechanics, 2003, **70**(7/8):pp. 927-941.

[2] Ohtsu, M., Okamoto, T. and Yuyama, S. *Moment Tensor Analysis of AE for Cracking Mechanisms in Concrete,* ACI Structural Journal, 1998, **95**(2): pp. 87-95.

[3] Ohtsu, M. and Yoshimura, S. *Analysis of Crack Propagation and Crack Initiation due to Corrosion of Reinforcement,* Construction and Building Materials, 1997, **11**(7-8): pp. 437-442.

[4] Ohtsu, M. and Uddin, F. A. K. M. *Mechanisms of Corrosion-Induced Cracks in Concrete at Meso- and Macro-Scales*, 2008, **6**(3):419-429.

[5] Erdogan, F. and Sih, G. C. *On the Crack Extension in Plates under Plane Loading and Transverse Shear,* J. Basic Engineering, 1963, **12**: pp. 519-527.